

## High-pressure study of ferromagnetic $U_xM_{1-x}$ (M = Pt, Ir) compounds

This article has been downloaded from IOPscience. Please scroll down to see the full text article.

2001 J. Phys.: Condens. Matter 13 5675

(<http://iopscience.iop.org/0953-8984/13/24/312>)

View [the table of contents for this issue](#), or go to the [journal homepage](#) for more

Download details:

IP Address: 171.66.16.226

The article was downloaded on 16/05/2010 at 13:33

Please note that [terms and conditions apply](#).

# High-pressure study of ferromagnetic $U_xM_{1-x}$ ( $M = \text{Pt}, \text{Ir}$ ) compounds

E D Bauer, E J Freeman, C Sirvent and M B Maple

Department of Physics and Institute For Pure and Applied Physical Sciences,  
University of California, San Diego, La Jolla, CA 92093, USA

Received 4 April 2001, in final form 4 May 2001

## Abstract

Measurements of the electrical resistivity under pressure to 20 kbar and the magnetization and specific heat at zero pressure were performed on the itinerant ferromagnetic compounds  $U_x\text{Pt}_{1-x}$  ( $0.50 \leq x \leq 0.54$ ) and  $\text{UIr}$ . The  $U_x\text{Pt}_{1-x}$  materials order magnetically at  $T_{C1} \sim 18$  K and  $T_{C2} \sim 27$  K and the ordering temperatures exhibit a small pressure dependence. Above 10 kbar, only the lower-temperature phase is present. The Curie temperature of  $\text{UIr}$ , on the other hand, decreases from 47 K at ambient pressure to 27 K by 19 kbar, and the critical pressure  $P_C$  for the complete suppression of ferromagnetism is estimated to be  $\sim 40$  kbar.  $\text{UPt}$  and  $\text{UIr}$  obey the Kadowaki–Woods relation and have Wilson ratios of order unity and could be classified as moderately heavy-fermion ferromagnetic materials.

## 1. Introduction

Matthias and co-workers discovered ferromagnetism in  $\text{UPt}$  over 30 years ago and a great deal of research has been carried out on this intriguing compound since then [1–6].  $\text{UPt}$  has a U–U separation of 3.6 Å which is very close to the distance of 3.5 Å above which Hill proposed direct 5f orbital overlap would be negligible [7]. Therefore,  $\text{UPt}$  is close to the itinerant/localized crossover, so some of its properties reflect the itinerant nature of the f electrons and other properties reflect more localized f-electron behaviour. Huber *et al* reported nearly complete suppression of the small saturation magnetization ( $\sim 0.45 \mu_B/\text{U atom}$ ) with pressures of 20 kbar, a nonmonotonic variation of the saturation magnetization with Pt concentration, and a nearly pressure-independent Curie temperature  $T_C$  of  $\sim 30$  K [2]. These phenomena, as well as large values of the electronic specific heat coefficient  $\gamma$  of  $100 \text{ mJ mol}^{-1} \text{ K}^{-2}$  [8] consistent with XPS studies [9], are best viewed in an itinerant-electron model. Other measurements such as those indicating a metamagnetic transition between 2–4 T at 4.2 K [10] and Curie–Weiss behaviour at high temperatures [2, 8] are most easily described in a local moment framework.

A number of studies of  $\text{UPt}$  revealed a second phase transition at  $\sim 19$  K in addition to the ferromagnetic one observed at 27 K. The appearance of a peak at 19 K in ac magnetic susceptibility measurements and a strong suppression of this transition in a magnetic field

of 5 T show that it is magnetic in origin [10]. X-ray diffraction experiments concluded that UPt, like UIr, forms in the monoclinic PdBi structure [11]. From neutron diffraction measurements, Frings *et al* found evidence of two ferromagnetic phases: one phase with a  $T_C$  of  $\sim 30$  K which crystallized in the PdBi structure, and another phase with a  $T_C$  of  $\sim 19$  K with an unknown structure that transforms under pressure to the PdBi phase, consistent with the decrease in magnetic moment with pressure [12]. A very recent study of UPt involving magnetization and resistivity measurements under pressure indicates a ferromagnetic phase at  $\sim 28$  K which disappears at  $\sim 15$  kbar and an antiferromagnetic phase at  $\sim 17$  K which persists up to  $\sim 40$  kbar [6]. Other work on tiny single crystals of UPt revealed a large anisotropy and a saturation moment of  $1 \mu_B/\text{U}$  atom with the easy direction along the  $b$ -axis of the monoclinic PdBi ( $P2_1$ ) structure and also the presence of an energy gap in the magnon dispersion curve giving rise to activated behaviour at low temperatures [4, 5].

The isomorphous compound UIr is also ferromagnetic with a Curie temperature of 47 K and a saturation moment of  $0.6 \mu_B/\text{U}$  atom along the  $b$ -axis [13, 14]. The U–U separation in this material is in the range of 3.3 to 3.9 Å, which is close to the Hill limit. The magnetic properties of UIr are similar to those of UPt in that they exhibit Curie–Weiss behaviour at high temperatures indicating local moment behaviour and reduced moment magnetism at low temperatures [14].

In this paper, we present measurements of electrical resistivity under applied pressures up to 20 kbar, magnetization, and specific heat on  $\text{U}_x\text{Pt}_{1-x}$  ( $x = 0.50, 0.52, 0.54$ ) and UIr. This work was partially motivated by the fact that the saturation moment of  $\text{U}_x\text{Pt}_{1-x}$  is almost completely suppressed with the application of 20 kbar of pressure [2], suggesting that the system might be approaching a magnetic instability. There has been a great deal of interest recently in non-Fermi liquid (NFL) materials, which have unusual low-temperature properties due to the proximity of a magnetic–nonmagnetic transition (see for example reference [15]). We found that in the  $\text{U}_x\text{Pt}_{1-x}$  compounds, the ferromagnetic transition(s) is (are) present at 20 kbar with little change in the Curie temperature. In contrast, the Curie temperature of UIr is rapidly suppressed with pressure, which is similar to the behaviour of other FM compounds such as MnSi [16], ZrZn<sub>2</sub> [16, 17], and UGe<sub>2</sub> [18].

## 2. Experimental details

Polycrystalline samples of  $\text{U}_x\text{Pt}_{1-x}$  for  $x = 0.50, 0.52, 0.54$  and UIr were prepared by arc melting stoichiometric amounts of pure elements U (3N7) and M ( $M = \text{Pt, Ir}$ ; 4N) in a Zr-gettered argon atmosphere. The samples were then wrapped in Ta foil with a Zr getter and annealed in evacuated quartz ampoules at 900 °C for one week. The x-ray diffraction patterns are consistent with the PdBi-type structure [12–14, 19] for the  $\text{U}_x\text{M}_{1-x}$  ( $M = \text{Pt, Ir}$ ) compounds, except for ThIr whose pattern corresponds to the orthorhombic CrB-type structure [20]. Electrical resistivity measurements were performed under hydrostatic pressure in a beryllium–copper piston–cylinder clamp device up to 20 kbar using Fluorinert FC75 as a pressure-transmitting medium. The resistivity was measured from a temperature of 1 K to 295 K using an ac resistance bridge operating at a frequency of 16 Hz and a current of 1–10 mA. The pressure was inferred inductively from the superconducting transition of a Pb manometer [21]. ac susceptibility measurements were made using a Quantum Design SQUID magnetometer in a field of 1 Oe at a frequency of 100 Hz from 5 to 60 K. dc susceptibility measurements were made in fields up to 55 kOe from 1.8 K to 295 K. Specific heat measurements were made in a <sup>3</sup>He calorimeter using a standard adiabatic heat-pulse technique.

### 3. Results

#### 3.1. Resistivity

The electrical resistivity  $\rho$  of  $U_{0.50}\text{Pt}_{0.50}$  from 1 to 295 K at applied pressures up to 17.8 kbar is shown in figure 1. In the paramagnetic region,  $\rho$  is nearly constant down to  $\sim 30$  K and decreases precipitously below  $\sim 30$  K, signalling the onset of ferromagnetism. The insets (a) and (b) of figure 1 show the resistivity and  $d\rho/dT$ , respectively, at various pressures below 40 K. Two phase transitions are observed, one at  $\sim 18$  K and the other at  $\sim 27$  K, identified as kinks in  $\rho$  and by the increase in  $d\rho/dT$ , and denoted by the arrows at ambient pressure in figure 1. For pressures above  $\sim 10$  kbar, there appears to be only one phase transition at 18 K and the curves are very similar to each other, at least below 40 K. The two magnetic transitions do not change significantly with pressure. In the paramagnetic region, there is a maximum in  $\rho$  which moves to higher temperatures and broadens considerably with increasing pressure. The residual resistivity,  $\rho_0$ , decreases monotonically with pressure from  $18 \mu\Omega \text{ cm}$  at  $P = 0$  to  $10 \mu\Omega \text{ cm}$  at  $P = 17.8$  kbar.

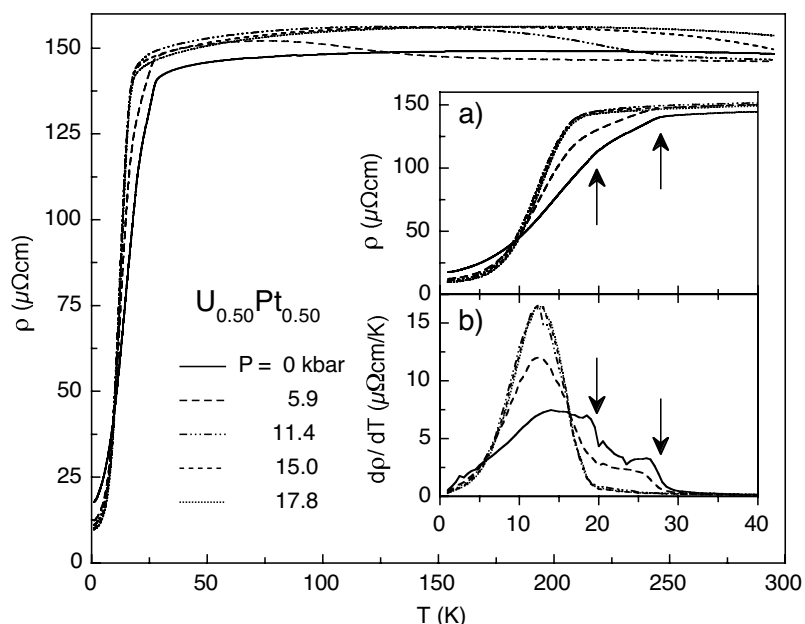


**Figure 1.** Electrical resistivity  $\rho$  versus temperature  $T$  for  $U_{0.50}\text{Pt}_{0.50}$  at various applied pressures. Inset (a):  $\rho$  versus  $T$  below 40 K. Inset (b):  $d\rho/dT$  versus  $T$ . Note the upturns at 19 K and 28 K indicating the ferromagnetic phase transitions (the arrows correspond to two ferromagnetic transitions at ambient pressure).

The resistivity  $\rho$  versus  $T$  for  $U_{0.52}\text{Pt}_{0.48}$  at various applied pressures is shown in figure 2. The pressure dependence of the ordering temperatures at  $\sim 18$  K and  $\sim 27$  K is small as shown in the plots of  $\rho$  and  $d\rho/dT$  in insets (a) and (b) of figure 2, respectively (the arrows correspond to the ambient pressure transitions). Two phase transitions are observed for pressures below  $\sim 10$  kbar, whereas only the lower transition is observed above 10 kbar, similar to the behaviour of  $U_{0.50}\text{Pt}_{0.50}$ . The resistivity has a broad maximum in the paramagnetic state which shifts to higher temperatures with pressure. The residual resistivity decreases monotonically with pressure from  $25 \mu\Omega \text{ cm}$  at  $P = 0$  kbar to  $17 \mu\Omega \text{ cm}$  at  $P = 19$  kbar.

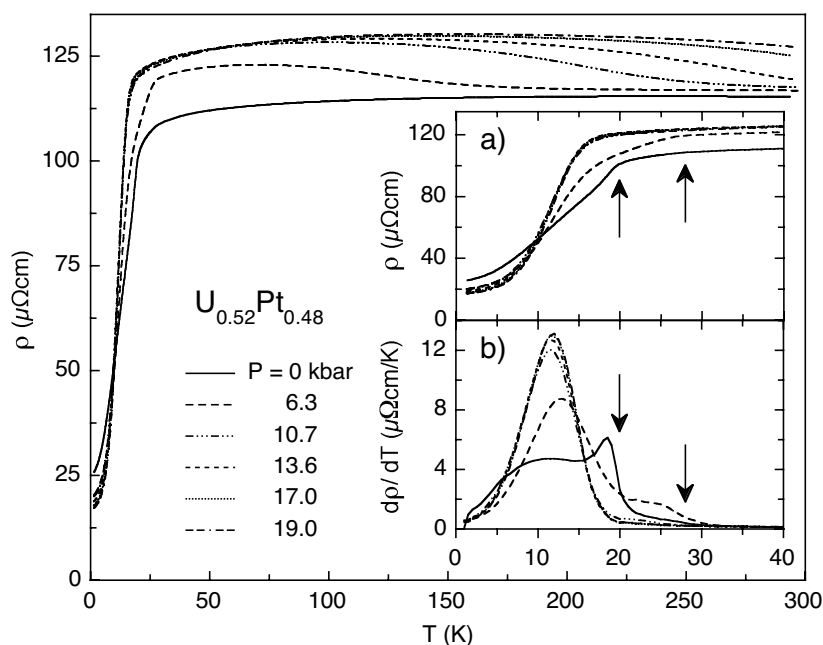


**Figure 2.** Electrical resistivity  $\rho$  versus temperature  $T$  for  $\text{U}_{0.52}\text{Pt}_{0.48}$  at various applied pressures. Inset (a):  $\rho$  versus  $T$  below 40 K. Inset (b):  $d\rho/dT$  versus  $T$ . Note the upturns at 19 K and 28 K indicating the ferromagnetic phase transitions (the arrows correspond to two ferromagnetic transitions at ambient pressure).

Displayed in figure 3 is  $\rho$  versus  $T$  for  $\text{U}_{0.54}\text{Pt}_{0.46}$  for a number of pressures up to 13.6 kbar. There are two anomalies in  $\rho$  at  $\sim 18$  K and  $\sim 27$  K at all pressures up to 13.6 kbar above which only the transition at  $\sim 18$  K is observed. Shown in insets (a) and (b) of figure 3 are plots of  $\rho(T)$  and  $d\rho/dT$  below 40 K. For  $\text{U}_{0.54}\text{Pt}_{0.46}$ , the measurements were not collected with increasing pressure steps, but were made at room temperature in the order denoted by the numbers beside each pressure. No hysteresis was observed near the phase transitions which suggests that the transformation between the two phases is reversible. However, there is a slight amount of hysteresis in the magnitude of the resistivity. Above 30 K, a hump-like feature is observed in  $\rho(T)$  which grows in magnitude and broadens considerably with pressure. The resistivity is nearly constant at temperatures above this hump, similar to the behaviour of the other  $\text{U}_x\text{Pt}_{1-x}$  compounds.

The resistivity  $\rho(T)$  versus  $T$  for  $\text{UIr}$  at various applied pressures is shown in figure 4. At ambient pressure, the onset of ferromagnetism is indicated by a kink in  $\rho$  and occurs at 47 K, in agreement with magnetization measurements discussed below and previous results [14, 22]. The ferromagnetism is suppressed to lower temperatures with applied pressure as shown in inset (a) of figure 4. To further describe the behaviour of  $\text{UIr}$ , the derivative,  $d\rho/dT$ , is shown in figure 4(b) below 60 K. One can see the large increase in  $d\rho/dT$  indicating the ferromagnetic transition. The Curie temperature  $T_C$  of 47 K of  $\text{UIr}$  corresponds well to the half-height of the  $d\rho/dT$  jump. With increasing pressure,  $T_C$  decreases and the transition becomes less sharp as indicated by the decrease in the magnitude of the jump in  $d\rho/dT$ . The Curie temperatures,  $T_{C1}$  and  $T_{C2}$ , for the  $\text{U}_x\text{Pt}_{1-x}$  compounds, and  $T_C$  for  $\text{UIr}$  versus applied pressure  $P$  are shown in figure 5. There is a small decrease of  $T_{C1}$  and  $T_{C2}$  for the  $\text{U}_x\text{Pt}_{1-x}$  compounds ( $dT_{C1}/dP = -0.2 \pm 0.1$  K kbar $^{-1}$  and  $dT_{C2}/dP = -0.3 \pm 0.1$  K kbar $^{-1}$ ) similar

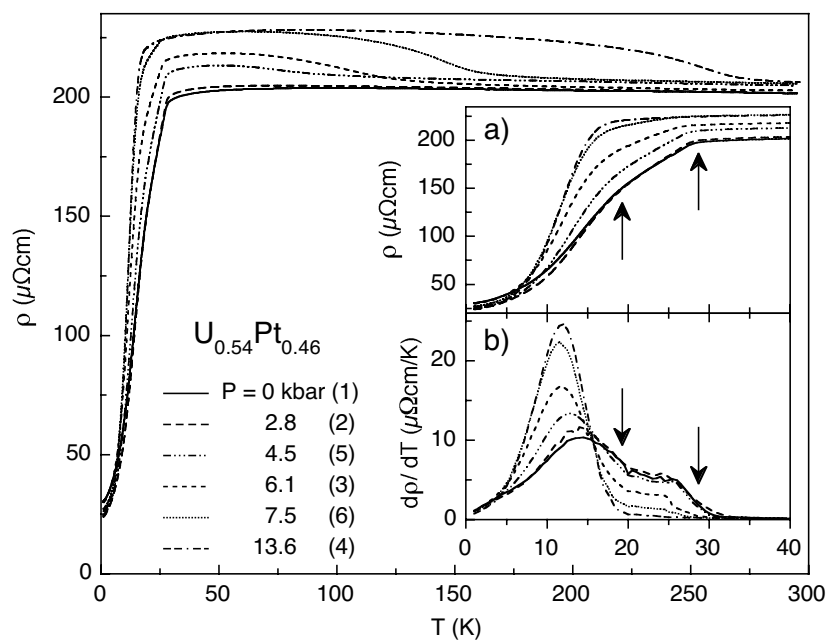


**Figure 3.** Electrical resistivity  $\rho$  versus temperature  $T$  for  $U_{0.54}Pt_{0.46}$  at various applied pressures. Inset (a):  $\rho$  versus  $T$  below 40 K. Inset (b):  $d\rho/dT$  versus  $T$ . Note the upturns at 19 K and 29 K indicating the ferromagnetic phase transitions (the arrows correspond to two ferromagnetic transitions at ambient pressure).

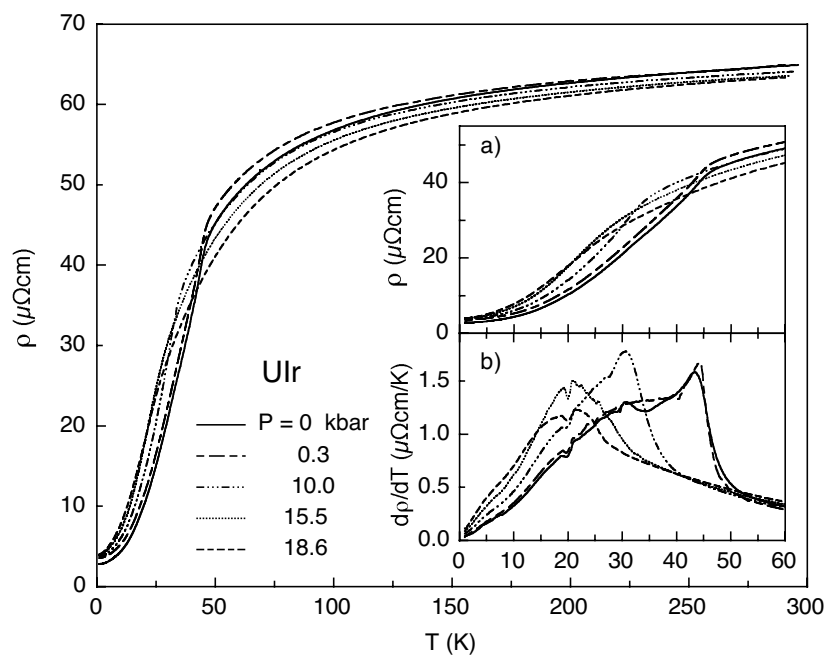


**Figure 4.** Electrical resistivity  $\rho$  versus temperature  $T$  for UIr at various applied pressures. Inset (a):  $\rho$  versus  $T$  below 60 K showing the suppression of the ferromagnetism with pressure. Inset (b):  $d\rho/dT$  versus  $T$ .

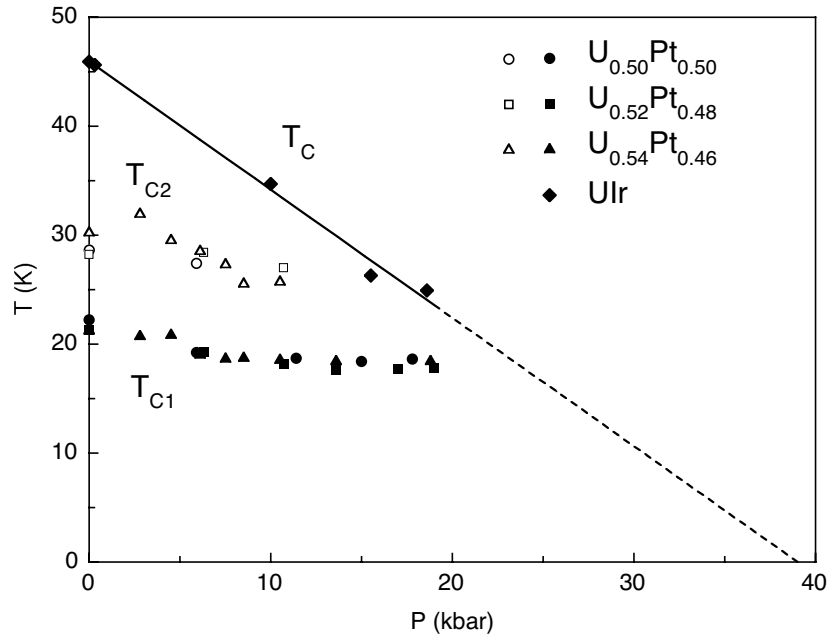


**Figure 5.** Curie temperatures  $T_{C1}$  and  $T_{C2}$  for the  $U_xPt_{1-x}$  compounds and  $T_C$  for UIr versus applied pressure  $P$ . The line is a fit to the Curie temperature data for UIr yielding a slope of  $dT_C/dP = -1.1 \text{ K kbar}^{-1}$ .

to previous measurements [2, 3, 6]. The Curie temperature of UIr decreases linearly with  $P$  at a rate  $dT_C/dP = -1.1 \text{ K kbar}^{-1}$  as indicated by the solid line in figure 5, and the critical pressure  $P_C$  is estimated to be  $\sim 40 \text{ kbar}$  by a linear extrapolation of the  $T_C$  versus  $P$  curve.

The resistivity  $\rho$  versus  $T^2$  for  $U_{0.50}Pt_{0.50}$  and UIr at various pressures is shown in figures 6(a) and 6(b), respectively. For  $U_{0.50}Pt_{0.50}$ ,  $\rho$  exhibits a  $T^2$ -dependence from 1 to 11 K at ambient pressure and over a smaller range of 1–5 K at higher pressures. Least-squares fits of the expression  $\rho = \rho_0 + AT^2$  to the data are indicated by the solid lines, and the results are listed in table 1. The value  $A = 0.27 \mu\Omega \text{ cm K}^{-2}$  for  $U_{0.50}Pt_{0.50}$  at ambient pressure is comparable to previously reported values of 0.19 [3], 0.45 [23], and  $0.30 \mu\Omega \text{ cm K}^{-2}$  [24]. The resistivity under pressure has also been measured by Frings and Franse who found that  $A$  increases from  $0.19 \mu\Omega \text{ cm K}^{-2}$  at zero pressure to  $0.23 \mu\Omega \text{ cm K}^{-2}$  at 4.2 kbar [3]. We find that  $A$  decreases with increasing pressure up to the highest pressures of 18.6 kbar as shown in figure 7. The behaviour of  $U_{0.52}Pt_{0.48}$  is very similar to that of  $U_{0.50}Pt_{0.50}$ ; i.e.,  $A$  decreases with  $P$ , while a maximum in the  $A(P)$  curve is observed for the  $U_{0.54}Pt_{0.46}$  compound at about 6 kbar. We have no explanation for this behaviour, but similar results were also reported in reference [6]. It is possible that the low-temperature properties are governed by the amounts of the two magnetic phases initially present at ambient pressure and which also vary considerably in this pressure range. The resistivity of UIr also exhibits a  $T^2$ -dependence from 1 to 12 K for pressures up to 15.5 kbar, and, at 18.6 kbar, the temperature range of the  $T^2$ -behaviour is reduced to 1–8 K (figure 6(b)). Prokeš *et al* observed an exponential dependence of the electrical resistivity and specific heat at low temperature of polycrystalline [4] and single crystals [5] of UPt which they attributed to an energy gap in the ferromagnetic magnon dispersion relation. They were able to fit the resistivity to the expression

$$\rho = \rho_0 + AT^2 + ET(\Delta + 2T)e^{-\Delta/T} \quad (1)$$

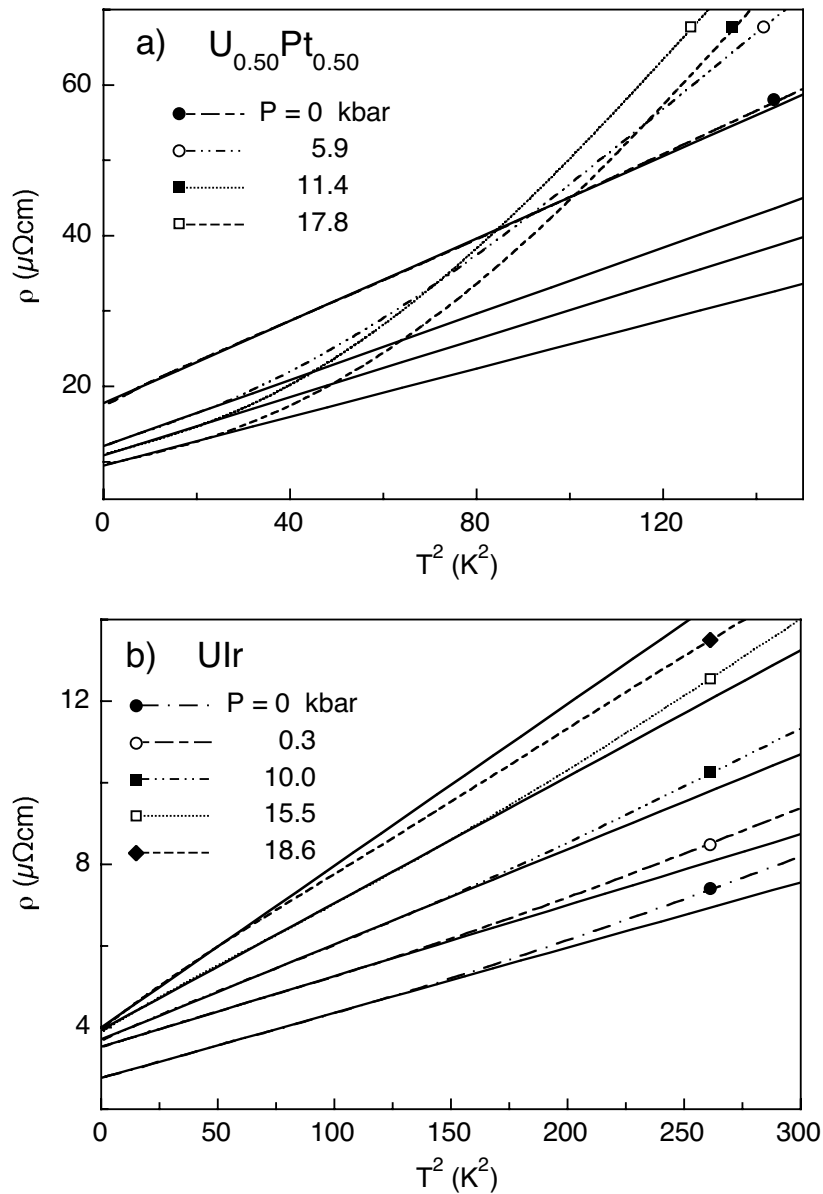


**Figure 6.** Panel (a):  $\rho$  versus  $T^2$  for  $U_{0.50}Pt_{0.50}$  at various applied pressures. Panel (b):  $\rho$  versus  $T^2$  for  $UIr$  at various applied pressures. In both panels, the solid lines are fits to the expression  $\rho = \rho_0 + AT^2$  of the  $\rho(T)$  data.

where  $E$  involves the electron–magnon coupling, and  $\Delta$  is the energy gap [25, 26]. Although our results are consistent with this spin-gap model, we have no supporting evidence for this behaviour from specific heat or magnetization measurements. Indeed,  $\rho$  follows a  $T^2$ -dependence over nearly a decade in temperature, at least at ambient pressure. It should be mentioned that the  $UPt$  samples studied by Prokeš *et al* were prepared by a different method to those used by other groups which did not observe exponential behaviour at low temperatures.



**Table 1.** Fitting parameters for the electrical resistivity of  $U_xM_{1-x}$  ( $M = \text{Pt, Ir}$ ) obtained from fits of the expression  $\rho = \rho_0 + AT^2$  to the  $\rho(T)$  data at various applied pressures. The uncertainties in  $A$  and  $\rho_0$  are estimated to be  $\Delta A = \pm 0.02 \mu\Omega \text{ cm K}^{-2}$  and  $\Delta\rho_0 = \pm 0.3 \mu\Omega \text{ cm}$  for the  $U_x\text{Pt}_{1-x}$  compounds and  $\Delta A = \pm 0.002 \mu\Omega \text{ cm K}^{-2}$  and  $\Delta\rho_0 = \pm 0.2 \mu\Omega \text{ cm}$  for UIr, for the listed fit ranges.

	$P$ (kbar)	$A$ ( $\mu\Omega \text{ cm K}^{-2}$ )	$\rho_0$ ( $\mu\Omega \text{ cm}$ )	Fit range (K)
$U_{0.50}\text{Pt}_{0.50}$				
	0	0.27	17.8	1–11
	5.9	0.22	12.1	1–5
	11.4	0.19	10.8	1–5
	15.0	0.17	9.9	1–5
	17.8	0.16	9.5	1–5
$U_{0.52}\text{Pt}_{0.48}$				
	0	0.29	25.4	1–9
	6.3	0.23	19.6	1–7
	10.7	0.22	19.4	1–6
	13.6	0.21	18.2	1–6
	17.0	0.20	17.3	1–6
	19.0	0.20	16.6	1–6
$U_{0.54}\text{Pt}_{0.46}$				
	0	0.35	30.4	1–10
	2.8	0.33	23.9	1–9
	4.5	0.37	24.2	1–7
	6.1	0.40	29.6	1–6
	7.5	0.38	26.8	1–5
	8.5	0.38	27.0	1–5
	10.5	0.36	28.4	1–5
	13.6	0.34	25.8	1–5
	18.8	0.32	23.8	1–5
UIr				
	0	0.016	2.8	1–12
	0.3	0.017	3.5	1–12
	10.0	0.023	3.7	1–12
	15.5	0.031	3.9	1–12
	18.6	0.040	4.0	1–8

As UPt involves a peritectic reaction of U and UPt<sub>2</sub>, it is perhaps not too surprising that there are a number of reports of slightly different physical properties, particularly with regard to the spin-gap behaviour mentioned above and also the value of the saturation moment.

### 3.2. Magnetization

The real part of the ac magnetic susceptibility  $\chi'_{ac}$  of  $U_xM_{1-x}$  ( $M = \text{Pt, Ir}$ ) is shown in figure 8 up to 60 K. Two peaks appear at  $\sim 19$  K and  $\sim 26$  K in the  $U_x\text{Pt}_{1-x}$  compounds for all concentrations, suggesting that two phases are present which is consistent with the resistivity measurements. It also appears that the magnitudes of  $\chi'_{ac}$  correspond well with the amounts of the two ferromagnetic phases, again in agreement with the resistivity results. For instance,  $U_{0.54}\text{Pt}_{0.46}$  has the largest amount of the 27 K phase, judging from the  $\chi'_{ac}$ -measurement, and

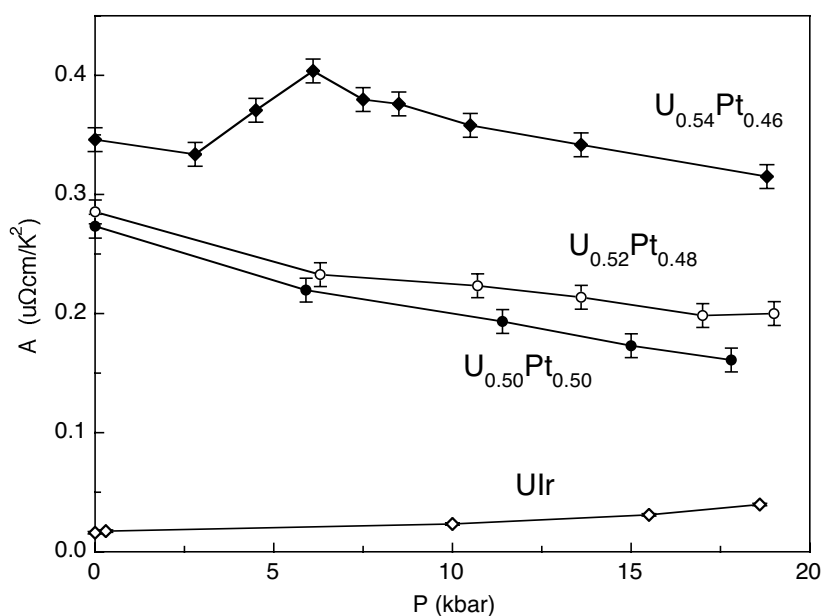


**Figure 7.** Coefficient  $A$  of the  $T^2$ -contribution to the electrical resistivity versus pressure  $P$  for  $U_xM_{1-x}$  ( $M = Pt, Ir$ ).

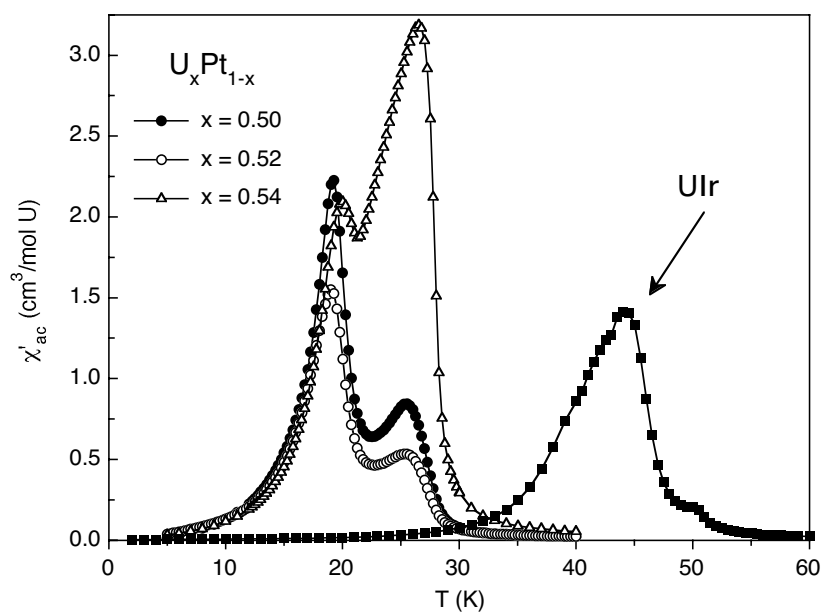


**Figure 8.** ac magnetic susceptibility  $\chi'_{ac}$  versus temperature  $T$  for  $U_xM_{1-x}$  ( $M = Pt, Ir$ ).

also shows a large decrease in  $\rho$  at that temperature. This is in contrast to  $U_{0.52}Pt_{0.48}$  which has a small amount of the 27 K phase and a small decrease of  $\rho$ . The Curie temperatures, identified as the peaks in  $\chi'_{ac}$  of the two phases, are nearly the same for all the  $U_xPt_{1-x}$  compounds, and

the results are listed in table 2. The ac magnetic susceptibility  $\chi'_{ac}$  for UIr also exhibits a peak at  $\sim 45$  K which corresponds to the  $T_C$  observed in  $\rho(T)$  and perhaps another one at  $\sim 50$  K. We ascribe this transition at 50 K to a minor impurity phase as there is no feature in the resistivity, dc magnetic susceptibility, or specific heat at that temperature.

**Table 2.** Magnetic properties of  $U_xM_{1-x}$  ( $M = \text{Pt, Ir}$ ). The Curie temperatures  $T_{C1}$  and  $T_{C2}$  of the two ferromagnetic phases for the  $U_xPt_{1-x}$  compounds are obtained from  $\chi_{ac}$ -measurements (the single  $T_C$  for UIr is also listed). The single Curie temperature  $T_C^{Arrott}$  is obtained from Arrott plots. The saturation moment  $\mu_s$ -values are obtained at  $T = 5$  K. The values of the effective moment  $\mu_{eff}$  and Curie–Weiss temperature  $\theta$  are determined from fits of the high-temperature magnetic susceptibility to a Curie–Weiss law.

Compound	$T_{C1}$ (K)	$T_{C2}$ (K)	$T_C^{Arrott}$ (K)	$\mu_s$ ( $\mu_B/\text{U atom}$ )	$\mu_{eff}$ ( $\mu_B$ )	$\theta$ (K)
$U_{0.50}Pt_{0.50}$	19.1	25.4	25	0.45	2.91	-214
$U_{0.52}Pt_{0.48}$	19.0	25.3	25	0.55	3.09	-132
$U_{0.54}Pt_{0.46}$	19.9	26.5	30	0.76	3.22	-141
UIr		44	47	0.31	2.91	-41

The dc magnetic susceptibility  $\chi$  ( $\equiv M/H$ ) versus  $T$  for  $U_xM_{1-x}$  ( $M = \text{Pt, Ir}$ ) in a magnetic field of  $H = 5$  kOe for temperatures below 100 K is shown in figure 9. There is a large upturn in  $\chi$  at  $\sim 30$  K for  $U_{0.54}Pt_{0.46}$  and at a somewhat lower temperature of  $\sim 25$  K for  $U_xPt_{1-x}$  ( $x = 0.50, 0.52$ ), signalling the onset of ferromagnetism. UIr shows similar behaviour but at  $\sim 50$  K. The fact that this upturn occurs at  $\sim 30$  K for  $U_{0.54}Pt_{0.46}$  indicates the strong presence of the higher-temperature ferromagnetic phase in this compound relative to the others, in accord with the resistivity and ac magnetic susceptibility results. At temperatures

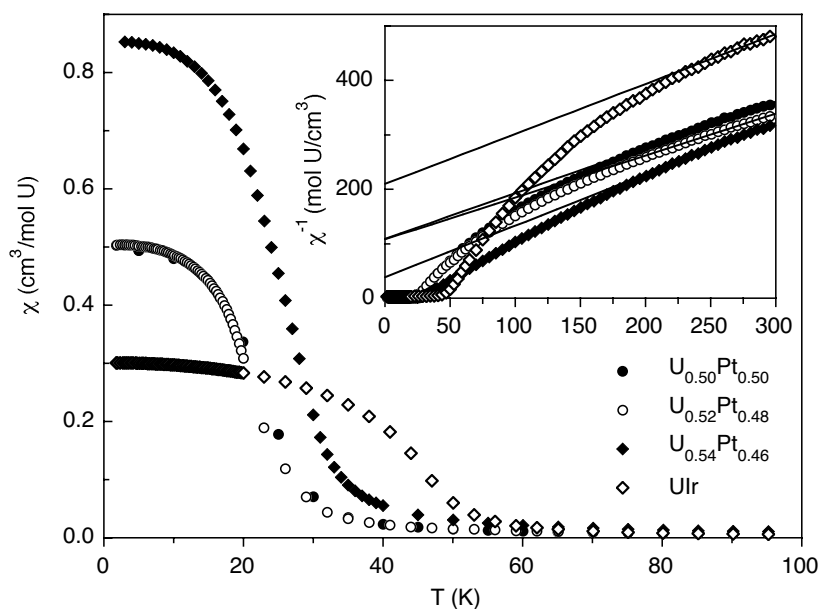


**Figure 9.** dc magnetic susceptibility  $\chi \equiv M/H$  versus temperature  $T$  for  $U_xM_{1-x}$  ( $M = \text{Pt, Ir}$ ) in a magnetic field of  $H = 5$  kOe. Inset: inverse magnetic susceptibility  $\chi^{-1}$  versus  $T$  for  $U_xM_{1-x}$  ( $M = \text{Pt, Ir}$ ). The lines are fits of a Curie–Weiss law to the  $\chi(T)$  data.

above 200 K, the magnetic susceptibility of the  $U_xM_{1-x}$  ( $M = \text{Pt, Ir}$ ) compounds can be described by a Curie–Weiss law

$$\chi = C/(T - \theta) \quad (2)$$

where  $C = N_A \mu_{eff}^2 / 3k_B$ ,  $\theta$  is the Curie–Weiss temperature, and  $\mu_{eff}$  is the effective moment in Bohr magnetons, although there is still significant curvature. Least-squares fits to a Curie–Weiss law displayed as  $\chi^{-1}$  versus  $T$  in the inset of figure 9 yield an effective moment  $\mu_{eff} \sim 3.0\text{--}3.2 \mu_B$ , smaller than what would be expected for a  $5f^2$  ( $\mu_{eff} = 3.57 \mu_B$ ) or  $5f^3$  ( $\mu_{eff} = 3.62 \mu_B$ ) configuration, and negative Curie–Weiss temperatures which could indicate the presence of crystalline electric fields or the Kondo effect (results collected in table 2). The full effective moment of  $\mu_{eff} = 3.6 \mu_B$  in  $U_{0.50}\text{Pt}_{0.50}$  and UIr is observed at temperatures above 600 K [8, 14, 27].

Magnetization measurements on  $U_xM_{1-x}$  ( $M = \text{Pt, Ir}$ ) were made at a number of fixed temperatures and are displayed as Arrott plots [28] ( $M^2$  versus  $H/M$ ) for  $U_{0.50}\text{Pt}_{0.50}$  and UIr in figures 10(a) and 10(b), respectively (open circles). The dashed lines are fits to the data yielding the square of the saturation magnetization  $M_{sat}^2$ . Plots of  $M_{sat}^2$  versus  $T$  are also shown in figures 10(a) and 10(b) (filled circles). The Curie temperatures, defined as the temperatures at which  $M_{sat}^2 \rightarrow 0$ , of 25 K and 47 K are obtained for  $U_{0.50}\text{Pt}_{0.50}$  and UIr, respectively. It is likely that the Curie temperatures obtained from this method correspond to the most prevalent ferromagnetic phase as  $T_C = 30$  K for  $U_{0.54}\text{Pt}_{0.46}$  and  $T_C = 25$  K for both  $U_{0.52}\text{Pt}_{0.48}$  and  $U_{0.50}\text{Pt}_{0.50}$ , similar to the values obtained from the magnetic susceptibility measurements. The saturation moment  $\mu_s$  at 5 K increases from  $0.45 \mu_B$  for  $x = 0.50$  to  $0.76 \mu_B$  for  $x = 0.54$  and  $0.31 \mu_B$  for UIr. The results for all of the  $U_xM_{1-x}$  ( $M = \text{Pt, Ir}$ ) compounds are listed in table 2.

### 3.3. Specific heat

Specific heat data for UIr and ThIr are shown in figure 11, plotted as  $C/T$  versus  $T$ . The ferromagnetic transition of UIr appears as a peak at  $\sim 45$  K. As displayed in figure 11(a), the specific heat of ThIr can be well described below 12 K by  $C/T = \gamma + \beta T^2$ , where  $\gamma$  is the electronic specific heat coefficient,  $\beta = 12\pi^4 r R / (5\theta_D^3)$  is the Debye phonon coefficient,  $r$  ( $=2$ ) is the number of atoms per formula unit,  $R$  is the universal gas constant, and  $\theta_D$  is the Debye temperature. Least-squares fits to the data yield  $\gamma = 1.5 \text{ mJ mol}^{-1} \text{ K}^{-2}$  and  $\theta_D = 173$  K. Below 10 K,  $C(T)$  of UIr has a small peak centred around 5 K perhaps due to a small content of magnetic impurities. Attempts to fit the specific heat of UIr to  $C = \gamma T + \beta T^3 + \alpha T^{3/2} + C_{imp}$ , where  $\alpha T^{3/2}$  is the contribution due to ferromagnetic magnons and  $C_{imp}$  (modelled by a Schottky anomaly) proved unsuccessful. We have therefore taken the phonon contribution to  $C(T)$  for ThIr as an approximation to the phonon contribution to  $C(T)$  for UIr, from which we have extracted a value of  $\gamma = 40 \text{ mJ mol}^{-1} \text{ K}^{-2}$  for UIr, as illustrated in inset (a) of figure 11. It should be mentioned that the value of  $\gamma$  obtained in this fashion is an estimate since the contributions to the specific heat due to magnons or impurities were not taken into account. However, if the magnon contribution of UIr is comparable to that of UPt ( $\alpha = 4 \text{ mJ mol}^{-1} \text{ K}^{-5/2}$  [3]), then this estimate of  $\gamma$  appears to be reasonable. The magnetic part of the specific heat was calculated by subtracting  $C(T)$  for ThIr and an electronic term  $\Delta\gamma = 38.5 \text{ mJ mol}^{-1} \text{ K}^{-2}$ , i.e.,  $C_{mag} = C(\text{UIr}) - C(\text{ThIr}) - \Delta\gamma T$ , and is shown in inset (b) of figure 11. The ferromagnetic transition of UIr at  $T_C \sim 47$  K is clearly seen, and there is also a small peak at 5 K which we attribute to a small content of an impurity phase. Assuming that the main contribution to the magnetic specific heat below 10 K is due to an impurity phase, the entropy associated with this peak is  $25 \text{ mJ mol}^{-1} \text{ K}^{-1}$  or 0.4% of  $R \ln 2$ . The magnetic

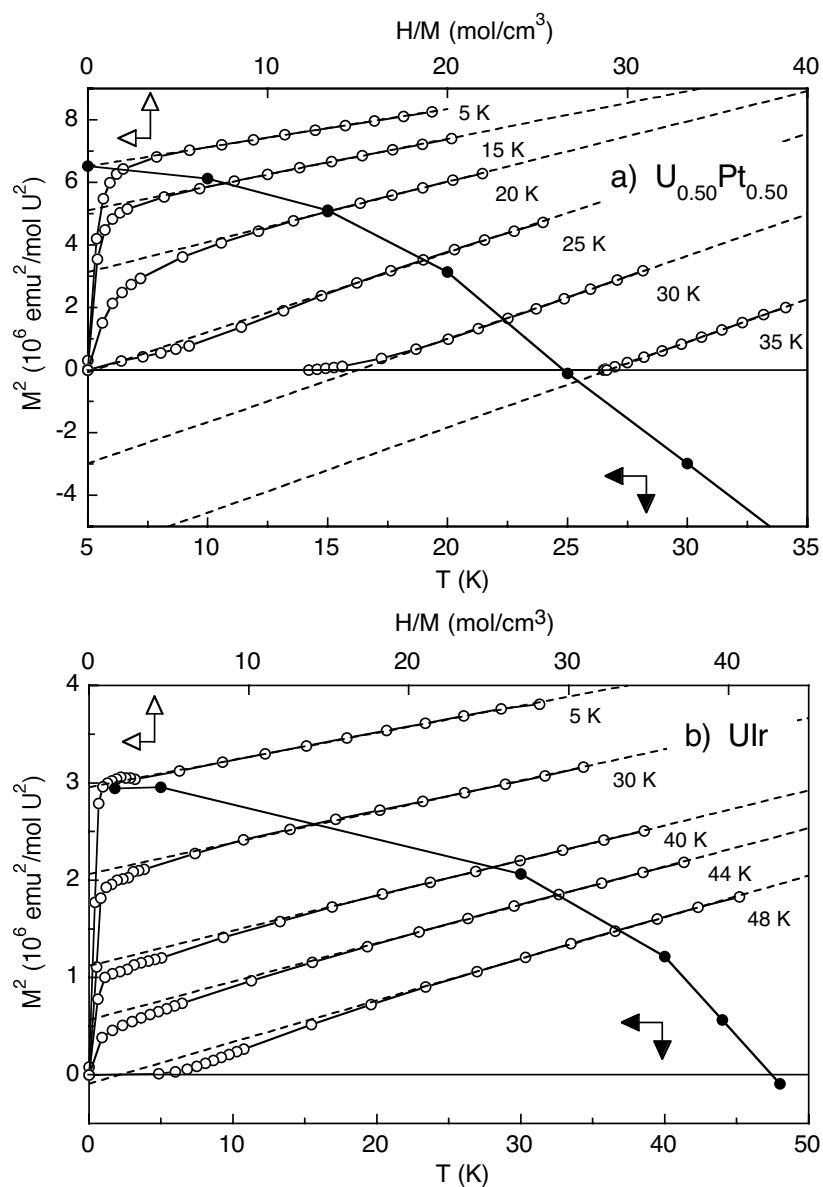


**Figure 10.** Panel (a): an Arrott plot ( $M^2$  versus  $H/M$ ) for  $\text{U}_{0.50}\text{Pt}_{0.50}$  (open circles). The dotted lines are fits to the data yielding the square of the saturation magnetization  $M_{sat}^2$ . The filled circles show  $M_{sat}^2$  versus temperature  $T$  yielding a Curie temperature of  $T_C = 25$  K. Panel (b): an Arrott plot of UIr (open circles). The dotted lines are fits to the data yielding the square of the saturation magnetization  $M_{sat}^2$ . The filled circles show  $M_{sat}^2$  versus temperature  $T$  yielding a Curie temperature of  $T_C = 47$  K.

entropy below 50 K amounts to  $575 \text{ mJ mol}^{-1} \text{ K}^{-1}$  (10% of  $R \ln 2$ ), neglecting the impurity contribution below 10 K. The enhanced electronic specific heat coefficient  $\gamma$  and the small amount of magnetic entropy of the ferromagnetism are consistent with the itinerant nature of the f electrons at low temperatures in this compound.

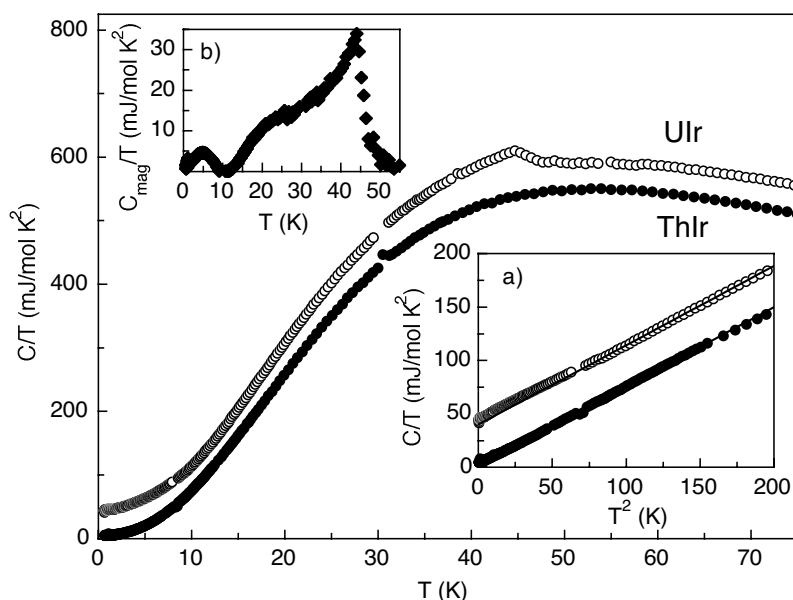


**Figure 11.**  $C/T$  versus  $T$  for UIr and ThIr. Inset (a):  $C/T$  versus  $T^2$  for UIr and ThIr. The lines are fits of the expression  $C/T\gamma + \beta T^2$  to the data. Inset (b): the magnetic contribution to the specific heat, plotted as  $C_{\text{mag}}/T$  versus  $T$ .

#### 4. Discussion

Our results show clear evidence for the presence of two magnetic phases, one at  $T_C \sim 19$  K (phase I) and the other at  $T_C \sim 27$  K (phase II), in the  $U_x\text{Pt}_{1-x}$  compounds, similar to what other groups have obtained, and our dc magnetization measurements suggest that the two phases are ferromagnetic in nature. Luengo *et al* found a  $T^{3/2}$ -contribution to the magnetic specific heat in UPt which is indicative of ferromagnetic magnons [29]. In addition, neutron diffraction measurements by Frings *et al* [12] suggest that the two phases are ferromagnetic. However, under the application of pressure, the diffraction lines of phase I show a marked decrease in intensity and they concluded that phase I transforms into phase II. Other ac magnetic susceptibility measurements on UPt under pressure yielded results similar to those obtained from the neutron diffraction study [27]. Contrary to these results, our electrical resistivity measurements under pressure suggest that the high-temperature phase (II) transforms into the low-temperature phase (I) with the application of  $P \sim 10$  kbar. Prokeš *et al* recently measured the magnetization and resistivity of UPt under pressure and also found evidence of two magnetic phase transitions. Their results indicate that phase II is ferromagnetic and is suppressed with the application of  $\sim 15$  kbar, while phase I is antiferromagnetic and is present up to  $\sim 40$  kbar, with the two phases coexisting between  $P = 15$  and 40 kbar. The results presented here are consistent with these findings, although the detailed behaviours of the resistivity may differ somewhat. We are not able to determine the exact nature of the lower-temperature phase, i.e., whether it is ferromagnetic or antiferromagnetic, from resistivity measurements alone. There is little change in the magnetic ordering temperatures with pressure in contrast to the findings for many other U-based compounds with magnetic ground states [30]. However, the isomorphous compound UIr exhibits a large decrease of the Curie temperature with pressure similar to other U compounds such as  $\text{UGe}_2$  [18].

In uranium intermetallic compounds, strong electronic correlations give rise to a wealth of different ground states. One of the key parameters governing the behaviour of these systems is the U–U separation which was pointed out by Hill [7]. In most of the U-based ferromagnets, the itinerant magnetism results mainly from 5f–5d/4d hybridization. A survey of UM (M = transition metal) compounds stresses the importance of the degree of hybridization and the number of valence electrons in determining the physical properties of these materials. URu is a Pauli paramagnet and UOs does not form. URh and UIr, with an additional valence electron, exhibit ferromagnetism at 57 K and 47 K with saturation moments  $\mu_s$  of 0.27 and 0.6  $\mu_B$ /U atom, respectively [14, 31]. UPd has not been studied in detail due to a limited temperature stability range and UPt has a  $T_C = 27$  K and  $\mu_s \sim 1 \mu_B$ /U atom [2, 4]. One possible explanation for the variation of the Curie temperature and the saturation moment is that the 5f–5d hybridization is decreased due to the shift of the 5d band to higher energies with increasing number of valence electrons. The physical properties of a number of pseudobinary U(M, M') systems are also consistent with this interpretation [14].

The low-temperature behaviour of the  $U_xM_{1-x}$  (M = Pt, Ir) compounds presented here is dominated by itinerant f electrons as indicated by the reduced saturation moment in the ferromagnetic state and the enhanced values of the electronic specific heat coefficient  $\gamma$ . A theory of spin fluctuations in itinerant-electron magnetism proposed by Moriya [32] predicts that the ratio of the paramagnetic effective moment,  $\mu_{eff}$ , to the saturation moment,  $\mu_s$ , should diverge as  $\mu_s$  or  $T_C \rightarrow 0$ , as  $\mu_{eff}$  is independent of  $\mu_s$  or  $T_C$ . This prediction can be illustrated by a Rhodes–Wohlfarth plot ( $\mu_{eff}/\mu_s$  versus  $T_C$ ) [33, 34]. The compounds  $U_xPt_{1-x}$  and UIr fall into the category of weak itinerant ferromagnets, with  $\mu_{eff}/\mu_s$  ratios of 6.5, 5.6, 4.2, and 9.4 for  $U_{0.54}Pt_{0.46}$ ,  $U_{0.52}Pt_{0.48}$ ,  $U_{0.50}Pt_{0.50}$ , and UIr, respectively. These values place the  $U_xPt_{1-x}$  materials between MnSi and  $Sc_3In$ , and UIr close to Pd–Co on a Rhodes–Wohlfarth plot. The heat capacities of  $U_{0.50}Pt_{0.50}$ ,  $U_{0.52}Pt_{0.48}$ , and the nonmagnetic analogue ThPt were measured by Luengo *et al* [29]. They determined the magnetic contribution to the heat capacity of  $U_{0.50}Pt_{0.50}$  by subtracting the lattice contribution of ThPt on the assumption that the electronic specific heat coefficients were comparable:  $\gamma(UPt) = \gamma(ThPt) = 3.5 \text{ mJ mol}^{-1} \text{ K}^{-2}$ . Frings and Franse reported a value of  $\gamma = 109 \text{ mJ mol}^{-1} \text{ K}^{-2}$  [3] that was confirmed by Prokeš *et al* [4], similar to those of other U–Pt compounds such as  $UPt_3$  and  $UPt_5$  [3] and also consistent with XPS measurements which found appreciable U 5f weight at the Fermi level [9, 35]. Our measurements on UIr yield an enhanced  $\gamma$  compared to that of ThIr. In the light of these facts, the strong electronic correlations in these materials may appear in the transport properties as a large value of the  $T^2$ -coefficient of the resistivity,  $A$ , as well as  $\gamma$ ; hence the  $U_xM_{1-x}$  (M = Pt, Ir) compounds might follow the Kadowaki–Woods relation  $A/\gamma^2 = 1 \times 10^{-5} \mu\Omega \text{ cm mol}^2 \text{ K}^2 \text{ mJ}^{-2}$  [36]. Using the values  $A = 0.27$  (0.016)  $\mu\Omega \text{ cm K}^{-2}$  and  $\gamma = 109$  (40)  $\text{mJ mol}^{-1} \text{ K}^{-2}$  for UPt (UIr), we calculate  $A/\gamma^2 = 2.8$  and  $1.0 \times 10^{-5} \mu\Omega \text{ cm mol}^2 \text{ K}^2 \text{ mJ}^{-2}$  for UPt and UIr, respectively. The other  $U_xPt_{1-x}$  materials also have comparable values of  $A$  and  $\gamma$  [2], so it seems likely that they also obey the Kadowaki–Woods relation. We calculated the Wilson–Sommerfeld ratio for the  $U_xM_{1-x}$  (M = Pt, Ir) compounds using the formula [37]

$$R_W = (\pi^2 k_B^2 / 3 \mu_{eff}^2) (\chi_0 / \gamma)$$

which is generally close to unity for heavy-fermion systems. We determined  $\chi_0$  from the high-field slope of the  $M(H)$  curves at 2 K. Using the values of  $\chi_0$  ( $\gamma$ ) of  $5.5 \times 10^{-3} \text{ cm}^3 \text{ mol}^{-1}$  (109  $\text{mJ mol}^{-1} \text{ K}^{-2}$ ) and  $5.2 \times 10^{-3} \text{ cm}^3 \text{ mol}^{-1}$  (40  $\text{mJ mol}^{-1} \text{ K}^{-2}$ ), we obtained  $R_W = 0.9$  and 2.2 for UPt and UIr, respectively. Similar values are expected for the other  $U_xPt_{1-x}$  materials studied here. Since UPt and UIr obey the Kadowaki–Woods relation and have Wilson ratios of order unity, it seems reasonable to classify them as moderately heavy-fermion materials.

## 5. Conclusions

The ferromagnetic compounds  $U_xPt_{1-x}$  and  $UIr$  were investigated by means of electrical resistivity measurements under pressure and magnetization and specific heat measurements at ambient pressure. The  $U_xPt_{1-x}$  compounds order magnetically at  $T_{C1} \sim 18$  K and  $T_{C2} \sim 27$  K, and the transition temperatures are suppressed only slightly with pressure. It appears that the higher-temperature phase transforms into the lower-temperature phase under pressure, and above 10 kbar, only the lower-temperature phase is present. The Curie temperature of  $UIr$  is more rapidly reduced with pressure, and the critical pressure for the suppression of ferromagnetism in this compound is estimated to be  $P_C \sim 40$  kbar.

## Acknowledgments

This work was supported by the US National Science Foundation under Grant No DMR-97-05454. One of us (CS) thanks the Spanish MEC for financial support.

## References

- [1] Matthias B T, Chu C W, Corenzwit E and Wohlleben D 1969 *Proc. Natl Acad. Sci. USA* **64** 459
- [2] Huber J G, Maple M B and Wohlleben D 1975 *J. Magn. Magn. Mater.* **1** 58
- [3] Frings P H and Franse J J M 1985 *J. Magn. Magn. Mater.* **51** 141
- [4] Prokeš K, Klaasse J C P, Hagmusa I H, Menovsky A A, Brück E H, de Boer F R and Fujita T 1998 *J. Phys.: Condens. Matter* **10** 10643
- [5] Prokeš K, Fujita T, Brück E, de Boer F R and Menovsky A A 1999 *Phys. Rev. B* **60** R730
- [6] Prokeš K, Mushnikov N V, Goto T, Tahara T, Ito M, Goto T, Makamura F, Fujita T, Hondo F and Oomi G 2000 *Phys. Rev. B* **62** 11527
- [7] Hill H H 1970 *Plutonium and Other Actinides* ed W N Miner (New York: AIME) p 1
- [8] Franse J J M, Menovsky A A, deVisser A, Frings P H and Vettier C 1987 *J. Magn. Magn. Mater.* **70** 351
- [9] Schneider W D and Laubschat C 1981 *Phys. Rev.* **23** 997
- [10] Franse J J M, Frings P H, de Boer F R and Menovsky A 1981 *Physics of Solids Under High Pressure* ed J S Schilling and R N Shelton (Amsterdam: North-Holland) p 181
- [11] Dommann A and Hulliger F 1988 *Solid State Commun.* **65** 1093
- [12] Frings P H, Vettier C, Dommann A, Hulliger F and Menovsky A 1989 *Physica B* **156+157** 832
- [13] Siegrist T, Page Y L, Gramlich V, Petter W, Dommann A and Hulliger F 1986 *J. Less-Common Met.* **125** 167
- [14] Dommann A, Hulliger F and Siegrist T 1987 *J. Magn. Magn. Mater.* **67** 323
- [15] See, for example, articles in Coleman P, Maple M B and Millis A J (ed) 1996 *Proc. Conf. on Non-Fermi Liquid Behaviour in Metals (Santa Barbara, CA, 1996)*; *J. Phys.: Condens. Matter* **8**
- [16] Julian S R, Carter F V, Grosche F M, Haselwimmer R K W, Lister S J, Mathur N D, McMullan G J, Pfeleiderer C, Saxena S S, Walker I R, Wilson N J W and Lonzarich G G 1998 *J. Magn. Magn. Mater.* **177-181** 265
- [17] Huber J G, Maple M B, Wohlleben D and Knapp G S 1975 *Solid State Commun.* **16** 211
- [18] Oomi G, Kagayama T and Ōnuki Y 1998 *J. Alloys Compounds* **271-273** 482
- [19] Lawson A C, Williams A, Huber J G and Roof R B 1986 *J. Less-Common Met.* **120** 113
- [20] Thomson J R 1962 *Nature* **194** 465
- [21] Smith T F, Chu C W and Maple M B 1969 *Cryogenics* **54** 53
- [22] Brändle H, Schoenes J and Hulliger F 1979 *Phys. Rev. B* **19** 384
- [23] Lawson A C 1970 *Phys. Lett. A* **33** 231
- [24] Tran V H and Troć R 2000 *Acta Phys. Pol.* **97** 399
- [25] Mackintosh A R 1963 *Phys. Lett.* **4** 140
- [26] Anderson N H and Smith H 1979 *Phys. Rev. B* **19** 384
- [27] Frings P H, Franse J J M, de Boer F R and Menovsky A 1983 *J. Magn. Magn. Mater.* **31-34** 240
- [28] Arrott A 1957 *Phys. Rev.* **108** 1394
- [29] Luengo C A, Maple M B and Huber J G 1975 *J. Magn. Magn. Mater.* **3** 305
- [30] Sechovský V and Havela L 1988 *Ferromagnetic Materials* vol 4, ed E P Wohlfarth and K H J Buschow (Amsterdam: North-Holland) p 309



- 
- [31] Ōnuki Y, Yun S W, Ukon I, Kobori A, Umehara I, Satoh K, Fukuhara T, Sato H and Takayanagi S 1992 *J. Phys. Soc. Japan* **61** 1751
  - [32] Moriya T 1985 *Spin Fluctuations in Itinerant Electron Magnetism* (Berlin: Springer)
  - [33] Rhodes P R and Wohlfarth E P 1963 *Proc. R. Soc.* **273** 247
  - [34] Wohlfarth E P 1978 *J. Magn. Magn. Mater.* **7** 113
  - [35] Schneider W D and Laubschat C 1980 *Phys. Lett. A* **75** 407
  - [36] Kadowaki K and Woods S B 1986 *Solid State Commun.* **58** 307
  - [37] Wilson K G 1975 *Rev. Mod. Phys.* **47** 773